CHAPTER III

THEORY

This chapter will be focused on laying theoretical ground work to be employed as a basis for interpretation of the experimental results. The principles of microfiltration are stated in section 3.1. In section 3.2, ultrasound and its applications are identified.

3.1 Principles of microfiltration

Microfiltration (MF) is a pressure-driven membrane separation technique for suspended macromolecules or macrosolute based on molecular size. It is well-suited to the separation of particles in the size range of 0.02 to 10 microns. Feed solution which is the substances to be concentrated or fractionated is forced through membrane under applied pressure between 1 and 5 bar as a driving force. Flowing over a membrane, larger substances comparing to membrane pore size, are retained while permeate, smaller substances, is removed [5].

There are two modes in which a microfiltration process can be undertaken, dead-end filtration and cross-flow filtration as shown in Figure 3-1. In dead-end filtration, mixture of solids and liquids is presented to the membrane at right angles to its surface. The retained solids build up into a cake layer causes an increased resistance to filtration and results declination in permeate flux. As a result, the dead-end filtration process must be terminated periodically to remove the retained particle or replace the filter medium. Unlike dead-end filtration, suspension in cross-flow filtration flows across the surface of the membrane. The liquid permeates through the membrane at right

angles to the direction of flow of the feed and the flow across the membrane surface sweeps away any accumulated solids, thereby keeping the membrane clear and maintaining high throughput rates [3].

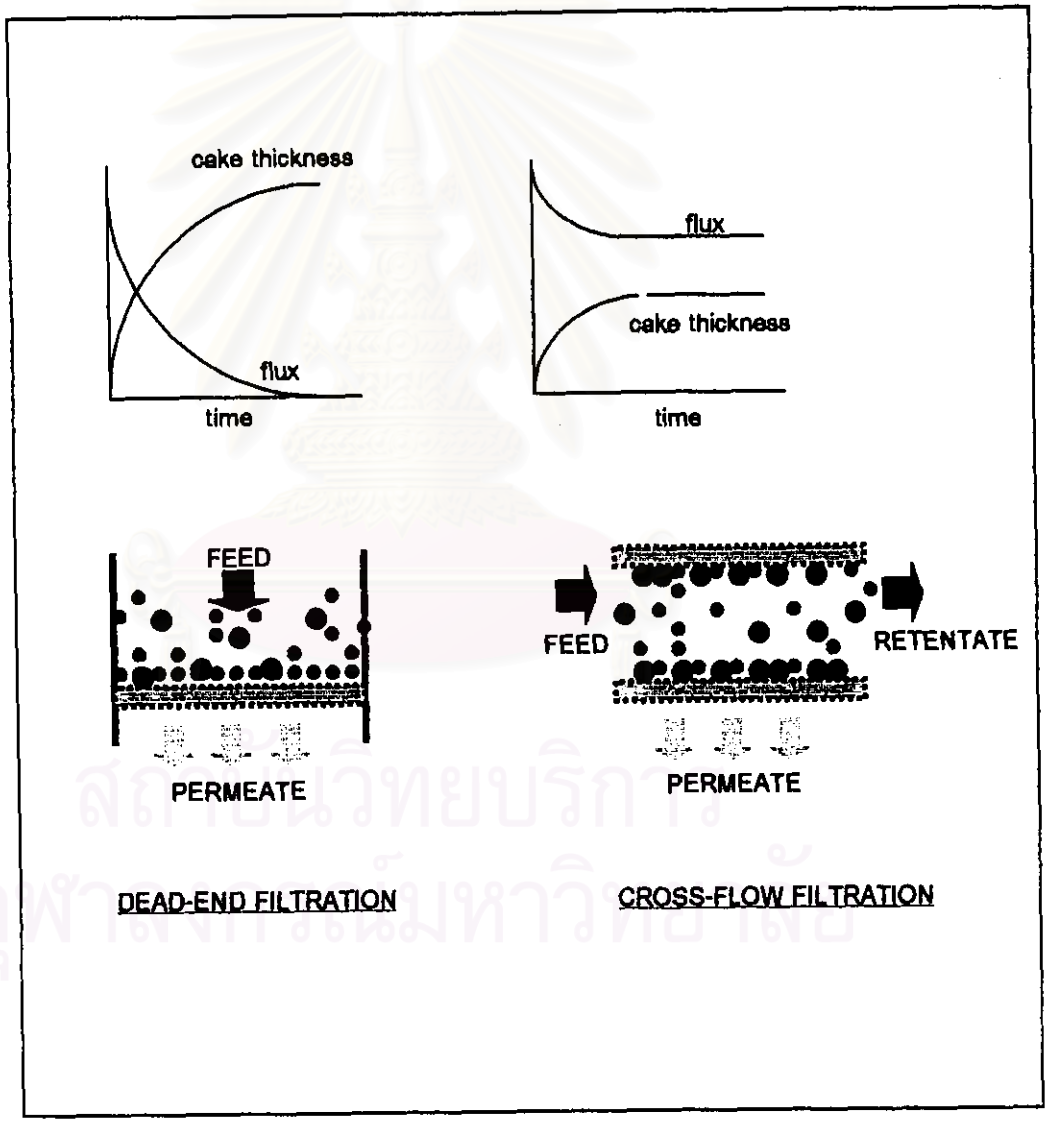

Figure 3-1: The schematics of dead-end filtration and cross-flow filtration

3.1.1 Mass transfer and gel polarization

As filtration occurs the retained macromolecule build up into a layer on the surface of membrane which causes resistance to the liquid flow. The macromolecule may move back into the bulk solution by natural diffusion and when the rate of solids being deposited at the membrane is counterbalanced by the rate of back diffusion, a concentration gradient of the macromolucule is set up at the membrane called "concentration polarization" as shown in Figure 3-2.

At steady state condition, the mass balance equation of solute concentration is affected by the convective mass transfer toward the membrane (JC) and the back diffusion movement (DdC/dx) as follows:

$$JC - (DdC/dx) = JC_p \qquad (3\text{-}1)$$

where

J = permeate flux ($cm^3/cm^2.s$),

C = concentration of macromolecule at x position (g/cm^3),

D = macromolecule diffusivity (cm^2/s),

x = fluid boundary layer thickness (cm),

C_p = concentration of macromolecule at permeate side (g/cm^3).

With the assumption of no macromolecule concentration at permeate side, the integration of Equation (3-1) beyond the boundary conditions of $C=C_b$ at $x=0$ and $C=C_w$ at $x=\delta$ yields:

$$J = D/\delta \ln (C_w/ C_b) \qquad (3\text{-}2)$$

or

$$J = k \ln (C_w/ C_b) \qquad (3\text{-}3)$$

where

δ = film thickness (cm),

k = mass transfer coefficient (cm/s),

C_w, C_b = concentration of macromolecule at the surface and in bulk fluid, respectively (g/cm^3).

In practice, as the flux increases, the value of C_w is increased as well and the maximum value of C_w is C_g where gel layer is formed so a mass balance equation for a gel formation, as shown in Figure 3-2 B, can be evaluated from substitution of C_w with C_g as follows:

$$J = k \ln (C_g / C_b) \quad (3\text{-}4)$$

When a gel layer is formed, the permeate flux logarithmically decreases with increasing macromolecule concentration in bulk fluid as the gel layer causes hydraulic resistance against flow and acts somewhat like a second membrane.

The mass transfer coefficient, k, depends on the driving pressure and any fluid flow across the membrane, can be illustrated in terms of dimensionless number as follows:

$$Sh = dk/D = ARe^{B}Sc^{1/3} \quad (3\text{-}5)$$

and

$$Re = (du\rho)/\beta \quad (3\text{-}6)$$

$$Sc = \beta/(\rho D) \quad (3\text{-}7)$$

where

d = fluid channel height over the membrane (cm),

A = constant number (-),

B = 0.5 (-) for laminar flow and 1.0 (-) for turbulent flow,

u = feed flow velocity (cm/s)

ρ = density of feed fluid (g/cm^3),

β = viscosity of feed fluid (g/cm.s),

Sh, Re, Sc = Sherwood number (-), Reynold number (-) and Schmidt number (-), respectively,

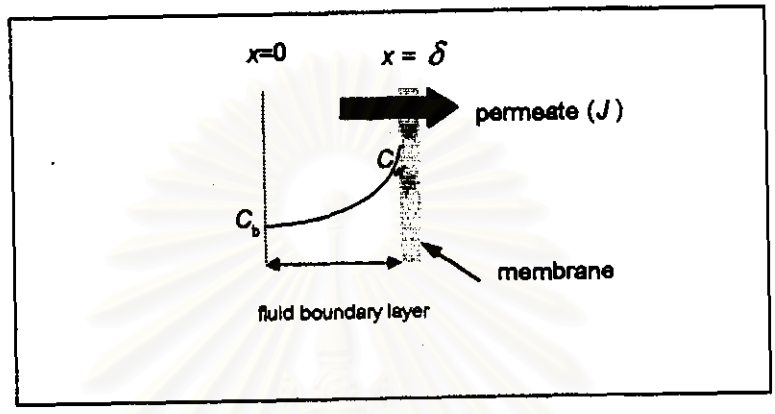

(A)

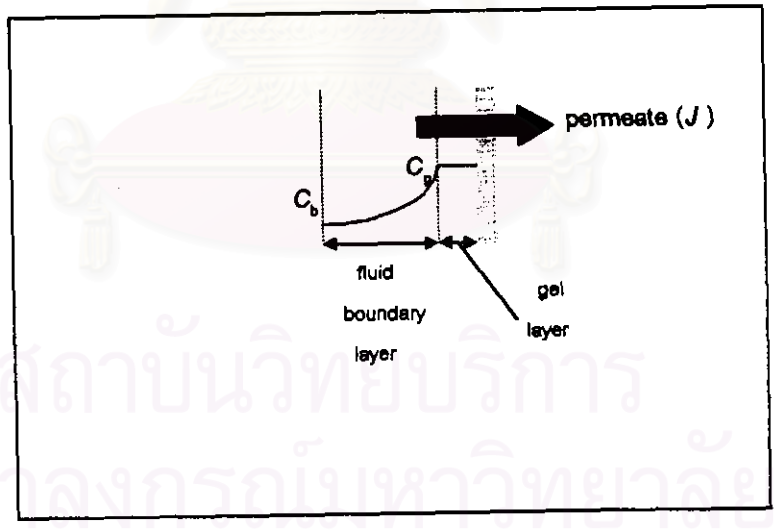

(B)

Figure 3-2 Concentration gradient in microfiltration

(A) without gel formation

(B) with gel formation

3.1.2 Cross-flow microfiltration principle

In cross-flow filtration, pressure is applied parallel to the membrane so that the macrosolute is swept away from the membrane, and therefore the thickness of the gel layer is reduced.

The main principle of cross-flow microfiltration is the fact that the feed flows tangentially with pressure difference as illustrated in Figure 3-3.

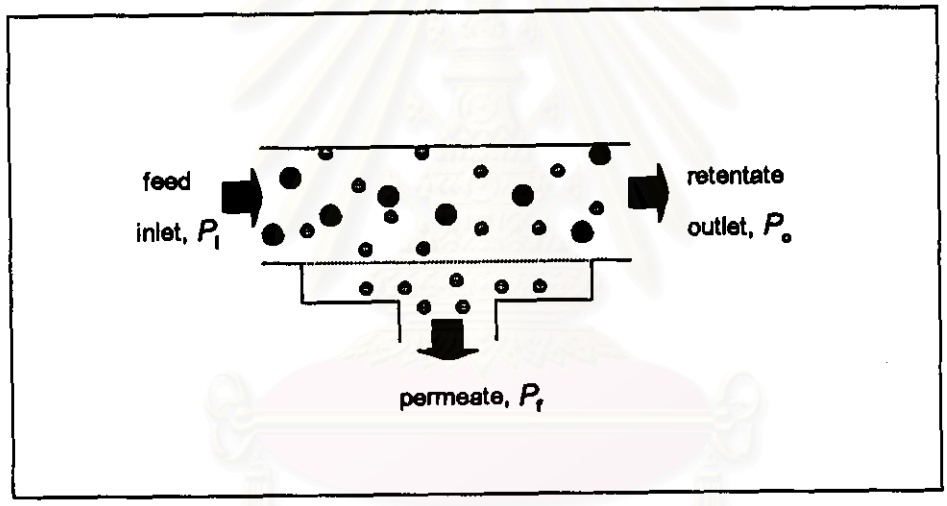

Figure 3-3 Cross-flow microfiltration model

Being a driving force, the pressure across the membrane (ΔP_{TM}) can be evaluated as follows:

$$\Delta P_{TM} = \{(P_i + P_o)/2\} - P_f \quad (3\text{-}8)$$

in case of permeating out at atmospheric pressure,

$$\Delta P_{TM} = \{(P_i + P_o)/2\} \quad (3\text{-}9)$$

where

ΔP_{TM} = transmembrane pressure drop (kPa),

P_i = pressure inlet the membrane (kPa),

P_o = pressure outlet the membrane (kPa),

P_f = pressure at the permeate side (kPa).

The permeate flux, which expresses the permeation performance, can be evaluated as:

$$J = \Delta P_{TM} / \mu R_t \quad (3\text{-}10)$$

$$R_t = R_m + R_c + R_p \quad (3\text{-}11)$$

where

J = permeate flux ($m^3/m^2.s$),

μ = viscosity of the solution (kPa.s),

R_t = total permeation resistance (1/cm),

R_m = membrane resistance (1/cm),

R_c = cake layer resistance (1/cm),

R_p = plugging resistance (1/cm).

Membrane resistance is constant in any membrane whereas cake layer resistance and plugging resistance varies with the macrosolute concentration and tangential velocity across the membrane which can retard or eliminate gel formation.

In conclusion, permeate flux of microfiltration depends on four parameters as follows:

1. Transmembrane pressure (ΔP_{TM}): Equation (3-9) and (3-10)

The permeate flux is proportional to transmembrane pressure up to the point when gel layer is formed. The further increase in pressure will increase the gel thickness until the constant permeate flux is achieved.

2. Feed flow velocity (u): Equation (3-4), (3-5) and (3-10)

Mass transfer coefficient is proportional to feed flow velocity. Moreover, increase in feed flow velocity will cause the sweeping of macromolecules over membrane surface by increasing shear force, therefore, gel layer and permeation resistance are decreased. Nevertheless, increasing feed flow velocity will decrease the average transmembrane pressure.

3. Concentration (C): Equation (3-4)

In general, the more solute concentration increases in feed solution, the less permeate flux is expressed which means the poorer filtration has occurred.

4. Temperature (T)

Being the function of temperature, mass transfer coefficient increases with temperature resulting in an increase of the permeate flux.

3.1.3 Membrane rejection

Membrane rejection can be expressed in term of rejection coefficient, σ, illustrated in Equation (3-12), which indicates the value in the range between 0-1. If complete filtration occurs, every solute is rejected across the membrane (C_p=0), the rejection coefficient will be 1. In contrast, when the rejection coefficient is zero, macrosolute is detected in permeate side. Therefore, membrane rejection is dependent on membrane selectivity and macrosolute concentration.

$$\sigma = 1-(C_p/C_b) \quad (3\text{-}12)$$

$$R = \sigma \times 100 \quad (3\text{-}13)$$

where

R = % rejection,

C_p, C_b = macromolecule concentrations in permeate and bulk solution, respectively.

3.1.4 Membrane configurations

There are four most common configurations for microfiltration membranes in industrial use: plate and frame unit, spiral cartridge, tubular modules and hollow fiber modules. In plate-and-frame systems, the membranes are attached to plates and the suspension flows across the membrane surface, while the permeate flows through the membrane to collection channels at the edge of the plate. The tubular module, consists of one or more membrane into a pressurized housing. In spiral cartridges, the membrane cloth is wrapped around a porous tube and fitted into a cylindrical vessel. The suspension flows parallel to the axis of the cylinder and the liquid permeetes through the central collection tube. The last one is a hollow fiber module, a bundle of hollow fiber membranes is contained within a shell. The suspension flows inside the hollow fibers and the permeate is collected in the shell side. The comparison of these configurations is expressed in Table 3-1.

Table 3-1 Comparison of MF membrane configurations.

Configurations	advantages	disadvantages
plate and frame	- simple design	- O-ring gasket seal problems - complex flow patterns
pleated cartridge	- large filtration area - good fluid distribution	- multiple materials of construction - difficult to clean
tubular	- convenient - easy to clean	- small filtration area
hollow fiber	- very high filtration area	- difficult to clean

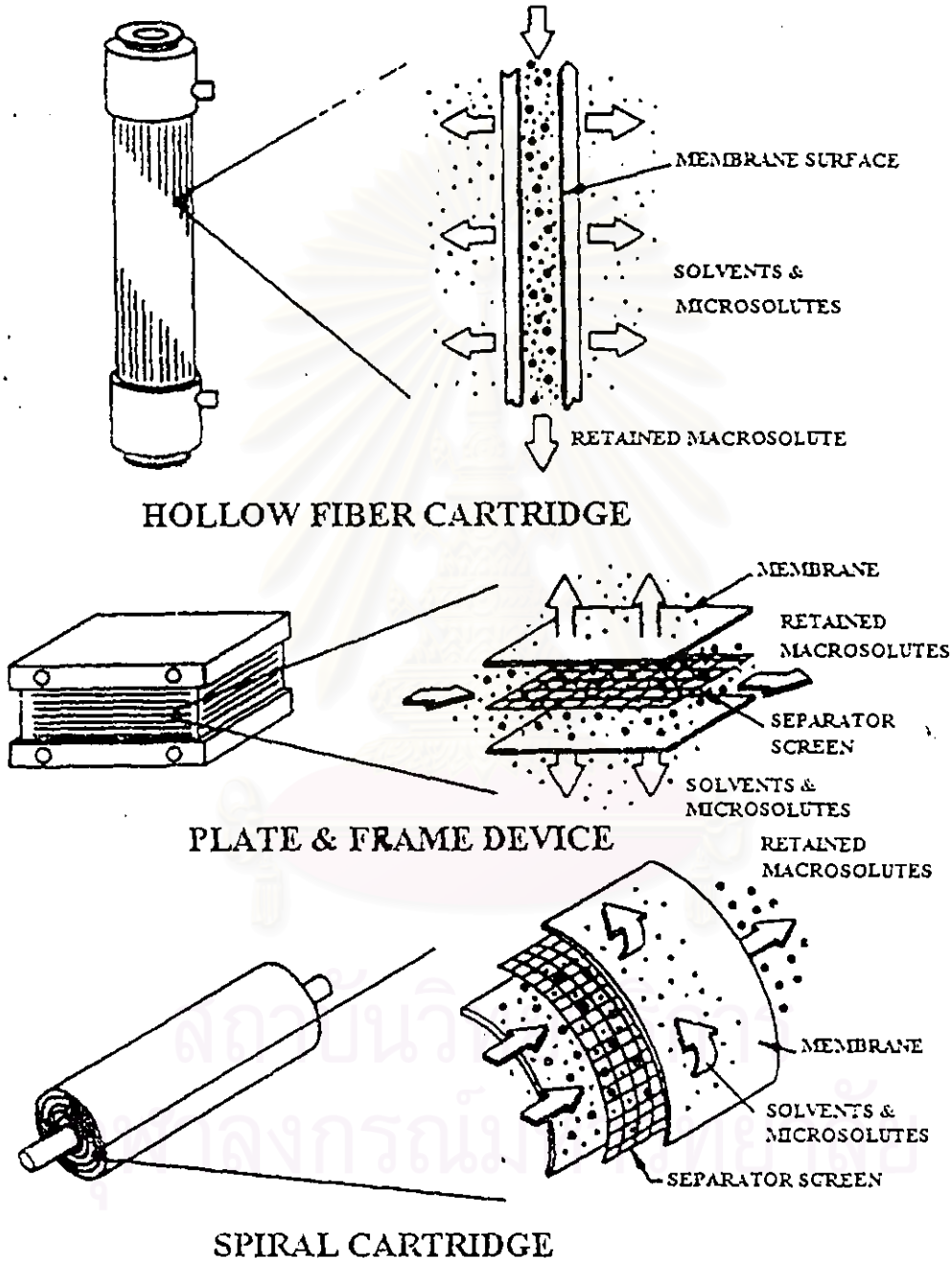

Figure 3-4: The examples of different membrane configurations

3.2 Sonochemistry, ultrasound and its applications

Sonochemistry, which was termed as the effect of ultrasound on chemical reactivity, has recently been an active area of research with many applications in chemical processes such as cleaning, sterilization, filtration, extraction, and etc.

Ultrasound is the sound wave having a frequency beyond that to which the human ear can respond: normally ranged between 20 kHz to 500 MHz. Ultrasound can be classified into 2 regions: power between 20 and 100 kHz and diagnostic between 1 and 10 MHz as shown in Figure 3-5. Some industrial uses of ultrasound are illustrated in Table 3-2. The applications of diagnostic ultrasound are not within the scope of the thesis, only the uses of power ultrasound which make significant effect to sonochemistry through the phenomenon of cavitation will be focused.

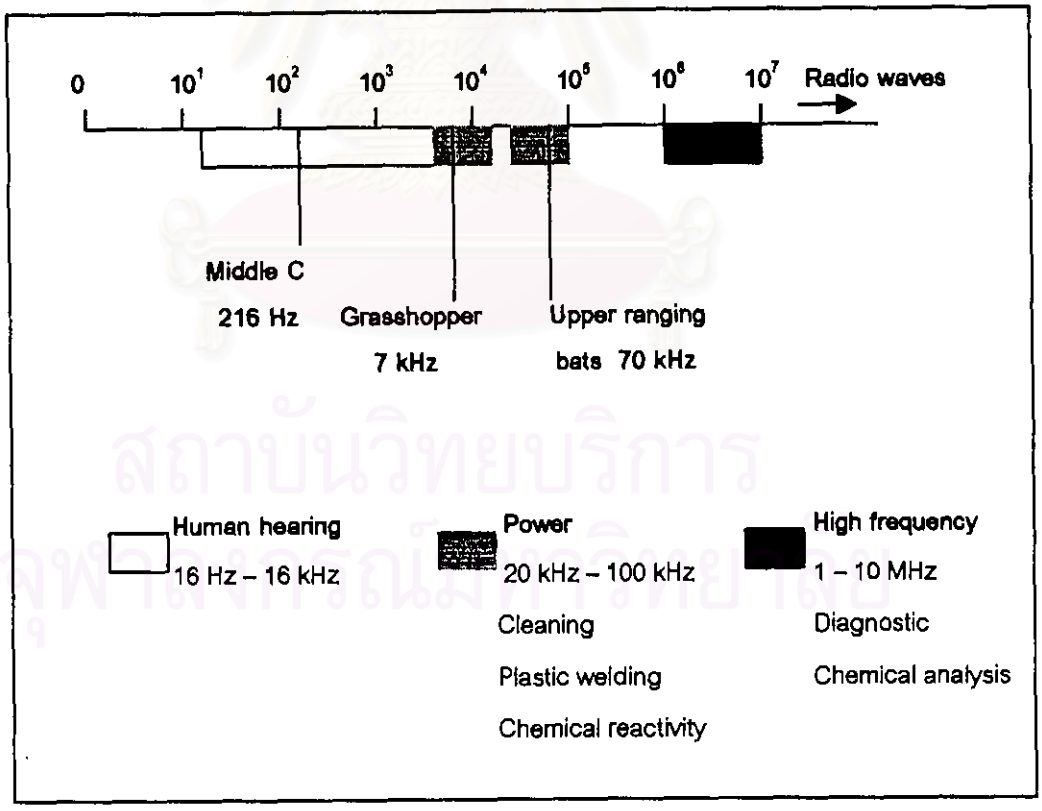

Figure 3-5: Sound frequencies

Table 3-2: Some industrial uses of ultrasound

Field	Application
Biology, Biochemistry	homogenisation and cell disruption
Engineering	drilling, grinding, and cutting
Dentistry	cleaning and drilling the teeth
Geography, geology	locating the mineral and oil deposits
Industrial	cleaning, particle dispersion
Medicine	observing the fetus
Plastics and polymers	initiating polymerization

3.2.1 Cavitation and its effects

Power ultrasound produces its chemical effects through the phenomenon of cavitation. When ultrasonic waves are propagated through a liquid medium in a series of compression and rarefaction, they will alternately compress and stretch the molecular structure of a medium, consequently, the average distance between the molecules will vary as the molecules oscillate about their mean position. If a sufficiently rarefaction pressure is applied, the distance between the molecules exceeds the critical molecular distance to hold the liquid intact, the liquid will break down and voids will be created, i.e., cavitation bubbles will form. The theory of bubble formation is expressed in Appendix A. Cavitation bubbles can be generated in two forms: stable and transient.

1. Stable cavitation

This type of bubbles is thought to mainly contain with gas or vapour and often non-linearly oscillates about some equilibrium size of many acoustic cycles due to the

irradiation conditions such as; frequency, intensity and hydrostatic pressure. These bubbles can either be transformed into transient bubbles or may continue to grow during subsequent cycles until they are sufficiently buoyant to float to the surface depends on the acoustic and environmental conditions of the medium.

2. Transient cavitation

Transient cavitation bubbles are voids, or vapour-filled bubbles which exist for one, or most a few acoustic cycles, expanding to a radius of at least twice their initial size, before collapsing violently on compression. With the assumption of adiabatic collapse of bubbles, allows for a calculation of the maximum temperature and pressure as within the bubble at the moment of total collapse follows:

$$T_{max} = T_0 [P_m(K-1)/P] \quad (3\text{-}14)$$

and

$$P_{max} = P [P_m(K-1)/P]^{K/(K-1)} \quad (3\text{-}15)$$

where

T_{max} = maximum pressure during the collapse (K),

T_0 = ambient (experimental) temperature (K),

P_{max} = maximum temperature during the collapse (kPa),

P = pressure in the bubble at its maximum size, usually assumed to be equal to the vapour pressure (P_v) of the liquid (kPa),

P_m = pressure in the liquid at the moment of transient collapse (kPa),

K = polytropic index of the gas (or gas vapour mixture).

As cavitation is necessary to induce sonochemical effects, therefore, the parameters which affect cavitation must be considered [6,7].

1. Effect of gas and particulate matter

The presence of gas and particulate matter in the liquid medium causes the lower liquid's tensile strength and this makes cavitation bubbles to be easily introduced. However, the cavitational collapse will be less violent with the presence of gas molecule in the liquid medium, represents in the less P_{max} and T_{max} (here the value of P in Equation (3-14) and (3-15) will be represented as $P_v + P_g$).

2. Effect of external pressure

The increase in applied pressure would lead to the raise of cavitation threshold due to the more dissolved gas occurred. This can be easily understood by the consideration of Equation (3-17). Any bubble, of radius R_0, within a liquid will remain in equilibrium if the supporting pressure within the bubble is equal to the crushing forces,

$$P_v + P_g = P_h + 2\sigma / R_0 \qquad (3\text{-}16)$$

If acoustic waves are introduced, the pressure within the liquid that causes the bubble to be expanded then becomes $P_h - P_a \sin(2\pi ft)$ and the bubble will grow (expand) when

$$P_v + P_g > P_h - P_a + 2\sigma / R_0 \qquad (3\text{-}17)$$

where .

P_a = acoustic pressure ($= \pm P_A \sin(2\pi ft)$; + in compression cycle, and – on rarefaction cycle) (kPa),

P_A = acoustic pressure amplitude (kPa),

P_g = pressure of gas within the bubble (kPa),

P_v = liquid vapour pressure (kPa),

σ = surface tension of the liquid medium (N/m).

Obviously, any increase in P_h (i.e. pressurize) results in the raise of cavitation threshold, and hence will require larger intensities (or P_a).

3. Effect of temperature

Generally, the threshold limit has been found to increase with decrease in temperature. As increase in temperature results in decreases in viscosity (η) and liquid surface tension (σ) whereas liquid vapour pressure (P_v) is increased, the bubble will be easily grown (Equation (3-17)), thereby the threshold is lower. Nevertheless, increase in temperature will also lessen the maximum temperature during the collapse as shown in Equation (3-14)).

4. Effect of intensity

The sound intensity is termed as the energy transmitted per second per square meter of fluid and can be represented as

$$\text{Intensity} = P_A^2 / 2\rho c \qquad (3\text{-}18)$$

where ρ is the density of the medium (g/cm^3) and c is the velocity of sound in that medium (m/s).

In general an increase in intensity will lower the time for bubble collapsing as can be seen from Equation (3-19) and provide for an increase in the sonochemical effects. However, it must be realized that intensity cannot be increased indefinitely, since the maximum bubble size, R_{max}, is also dependent upon the pressure amplitude as in Equation (3-20). With increase in the pressure amplitude (P_A) the bubble may grow so large on rarefaction (R_{max}) that the time available for collapse is insufficient.

$$\tau \approx 0.915 R_m (\rho / P_0)^{1/2} \qquad (3\text{-}19)$$

$$R_{max} = \frac{4}{3\omega_a}(P_A\text{-}P_h)(2/\rho P_A)^{1/2}[1 + \{2(P_A\text{-}P_h)/(3P_h)\}]^{1/3} \quad (3\text{-}20)$$

where

τ = cavity collapse time (s),

P_0 = constant ambient pressure (kPa),

R_m = radius of the cavity at the start of collapse,

ω_a = applied circular frequency (= $2\pi f_a$).

5. Effect of frequency

In order to achieve changes in chemical reactivity the frequencies between 20 to 50 kHz were applied to the liquid. At a very high frequency (diagnostic ultrasound), where that rarefaction cycles are very short, the finite time required for rarefaction cycle is too short to permit the bubble to grow to a size sufficient to cause disruption in the liquid. Even if a bubble was to be produced, the time required to collapse the bubble may be longer than is available in the compression-half cycle. The resultant cavitational effects, e.g. shock wave pressure, will therefore be less at the higher frequencies.

The mechanical and chemical effects of cavitation bubbles can separately be described in three cases:

1. Homogeneous system – involving a single liquid phase

Cavitation effects in a homogenous liquid will be felt in three distinct regions as illustrated in Figure 3-6:

(a) Inside the bubble, vapour from the solvent (or any volatile reagent present) will enter the bubble as cavitation bubble is being formed in the rarefaction cycle and will be subjected to the enormous increases in both temperature and pressure previously mentioned.

(b) At the interface between the bubble and the bulk liquid is a region where surface-active reagents may accumulate or where species produced in the bubble enter the liquid surface.

(c) In the liquid immediately surrounding the bubble an intense shock wave will be produced as liquid rapidly rushes into the volume previously occupied by the bubble and this will create enormous shear forces.

These mechanisms are differently used to induce sonochemical effects; (a) and (b) have been utilized to accelerate and enhance the reactions, while the fragmentation of particulate matter is introduced by (c).

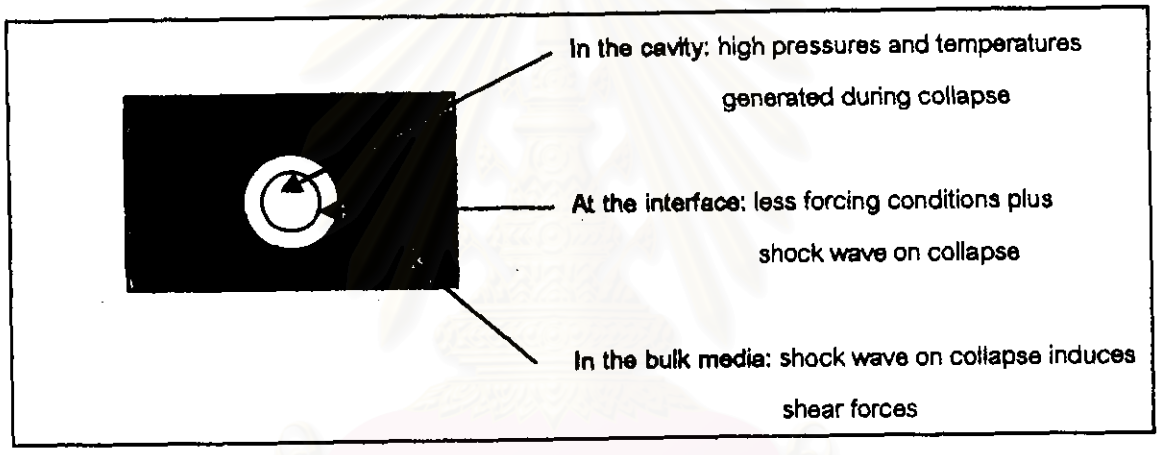

Figure 3-6: Cavitation effects in a homogenous liquid

2. Heterogeneous system – involving a solid and a liquid

Two types of cavitational collapse play significant effects on the surfaces of such solids as shown in Figure 3-7:

(a) Cavitational collapse on the surface itself which causes direct damage by the shock waves produced on implosion. These bubbles form on nuclei such as surface defects, impurities on the surface of the material or entrapped gas as illustrated in Figure 3-7 (a). This collapse is used to enhance the reactivity.

(b) Cavitational collapse close to a surface which does not produce a symmetrical shock wave. Instead a jet of solvent is generated which impinges on the surface

with great force and this phenomenon is the well known "cleaning action of ultrasound", expressed in Figure 3-7 (b).

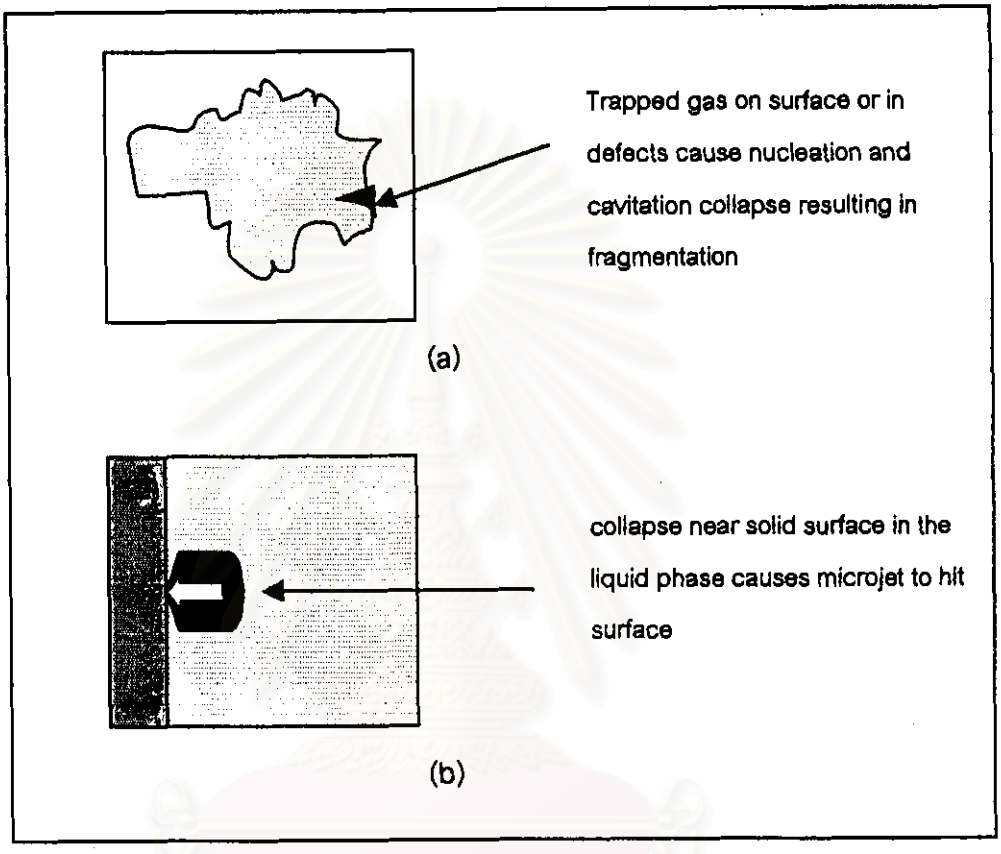

Figure 3-7: Cavitational effects at a solid/liquid interface

3. Heterogeneous system – involving immiscible liquids

Synthesis involving immiscible liquids (e.g. aqueous/ organic mixtures) can slowly occur since the reagents are often dissolved in different phases and the reaction between these species can only take place in the interfacial region between the liquids. However, sonication can be used to produce very fine emulsions from immiscible liquids via the cavitational collapse at or near the interface impels jets of one liquid into the other to form the emulsion as shown in Figure 3-8.

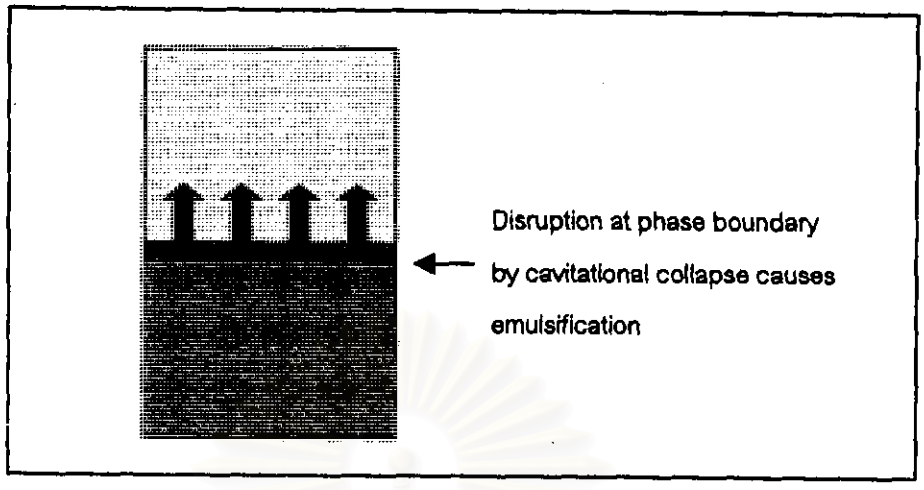

Figure 3-8: Cavitational effects at a liquid/liquid interface

3.2.2 Transducer: The generation of ultrasound

A transducer is the name for a device capable of converting one form of energy into another. There are two main types of ultrasonic transducers:

1. Mechanical transducer

This type of transducer converts kinetic energy of stream fluid into high frequency sound. The maximum frequency generated is 100 kHz.

2. Electromechanical transducer

This type of transducer converts electrical energy into high frequency sound. One popular example of this type is the piezoelectric transducer. It has many advantages such as a simple structure and easily applied to conventional chemistry equipment, so that found to have a widely used in many applications.

In operation, the signal generator provides high-voltage pulses of energy at the desired frequency to the transducer which converts electrical energy to acoustic energy based on piezoelectricity theory.

Piezoelectricity is the name for the phenomenon whereby electric dipoles are generated in certain anisotropic crystals when subjected to mechanical stress. It is particularly important that this phenomenon are reversible so consequently being also used as an acoustic detection [8]. The simplest piezoelectric transducer consists of a layer of piezoelectric ceramic with metal electrodes lay on both its surfaces. After applying an alternating electrical voltage, the thickness of the layer will change relating to the variation of the electrical field resulting in the generation of acoustic waves. With the requirements of a large radiating surface and a high intensity output, a composite or sandwich transducer has been developed. It is consisted of two pieces of piezoelectric ceramic clamped between two metals which are of different properties and dimensions as shown in Figure 3-9. Under electrical excitation, the piezoelectric ceramic is responsible for producing ultrasonic waves. The acoustic amplitude at the front surface of the transducer is amplified by the transmission line characteristic of the sandwich transducer and consequently high acoustic intensity is obtained. Lower intensity is obtained from the backing face due to its different sizes and properties.

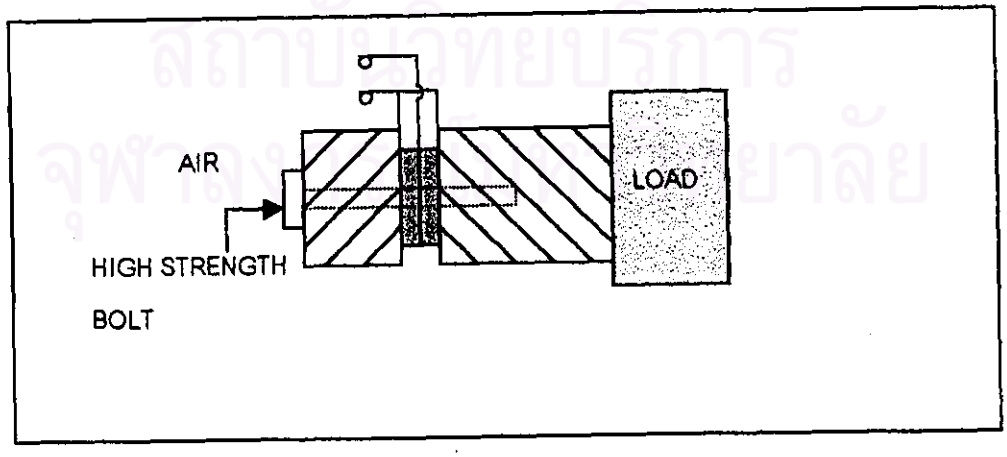

Figure 3-9: A composite transducer

The equivalent circuit of the piezoelectric transducer is expressed in Figure 3-10. The power input transferred to the transducer is

$$P = VI\cos\varphi \tag{3-21}$$

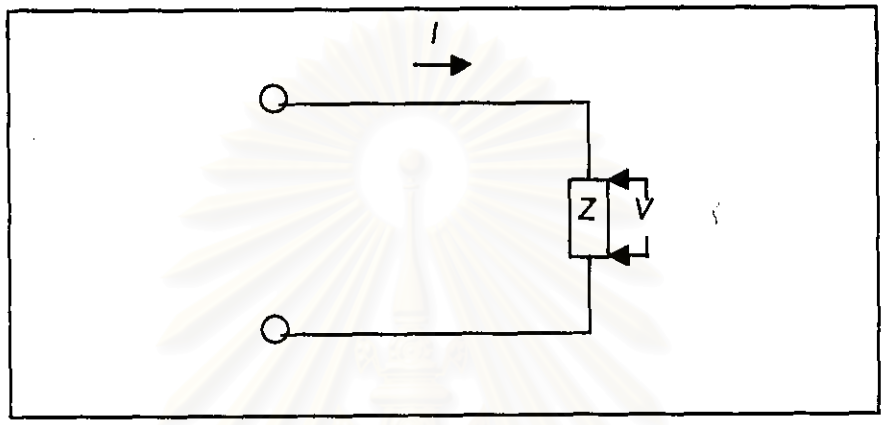

Figure 3-10: The equivalent circuit of the piezoelectric transducer

If all energy loss is ignored, the sound intensity obtained is

$$\text{Intensity} = P/A \tag{3-22}$$

where

P = input power (W),

V = voltage across the piezoelectric transducer (V),

I = current (amp.),

φ = the angle between the voltage and the current in the circuit (°),

A = area of irradiation surface (cm^2).

3.2.3 The waveform generated from a plane circular piston [9]

As the acoustic source used in our experiments is a piston source, the study of the waveform generated from a plane circular piston must be considered to investigate the propagation of an acoustic wave along the distance.

Assume a piston of radius a is mounted on a flat rigid battle of infinite extent. Let the radiating surface of the piston move uniformly with speed $U_0 \exp(j\omega t)$ normal to the baffle. The geometry and coordinates are sketched in Figure 3-11.

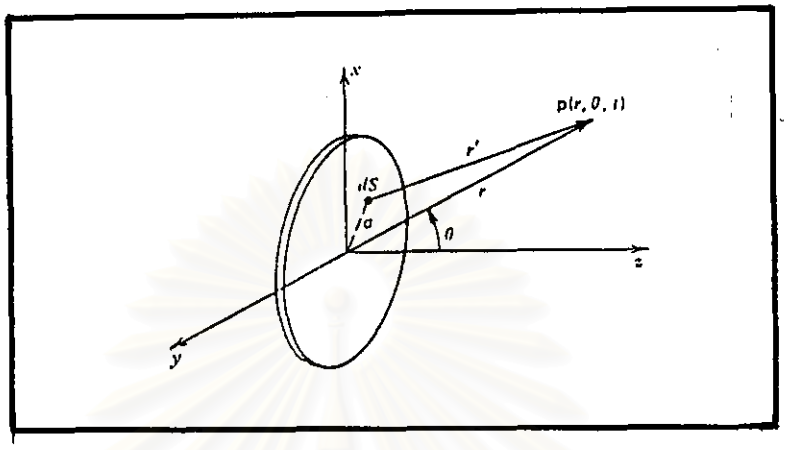

Figure 3-11: Geometry used in deriving the radiation characteristics of a flat piston

The total pressure generated is given by

$$p(r,\theta,t) = j\frac{\rho_0 c U_0 k}{2\pi}\int_S \frac{e^{j(\omega t - kr')}}{r'} dS \qquad (3\text{-}23)$$

where the surface integral is taken over the region $\sigma = a$.

The pressure amplitude on the axis of the piston is

$$P(r,0) = 2\rho_0 c U_0 \left| \sin\{\frac{1}{2}kr[\sqrt{1+\left[\frac{a}{r}\right]^2} - 1]\} \right| \qquad (3\text{-}24)$$

where $k = \omega / c = 2\pi / \lambda$.

Study of (3-24) reveals that the axial pressure exhibit s strong interference effects, fluctuating between 0 and $2\rho_0 c U_0$ as r ranges between 0 and ∞. These extremes of pressure occur for value of r satisfying

$$\{\frac{1}{2}kr[\sqrt{1+\left[\frac{a}{r}\right]^2}-1]\} = m(\pi/2) \quad \text{maxima: } m \text{ odd, minima: } m \text{ even} \qquad (3\text{-}25)$$

where $m = 0, 1, 2, 3, \ldots$. Solution of the above for the values of r at the extrema yields

$$\frac{r_m}{a} = \frac{1}{m}\frac{a}{\lambda} - \frac{m}{4}\frac{\lambda}{a} \qquad (3\text{-}26)$$

Moving in toward the source from large r, one encounters the first local maximum in axial pressure at $m = 1$, for which

$$\frac{r_1}{a} = \frac{a}{\lambda} - \frac{1}{4}\frac{\lambda}{a}$$

For still smaller r, the pressure amplitude falls to another minimum at $m = 2$, for which

$$\frac{r_2}{a} = \frac{1}{2}(\frac{a}{\lambda} - \frac{\lambda}{a})$$

and this continues to fluctuate between 0 and $2\rho_0 cU_0$ until the face of the piston is reached. A sketch of this behaviour is shown in Figure 3-12.

Thus, for values of r greater than r_1, the axial pressure displays a monotonically decreasing behaviour going asymtotically to a $(1/r)$ dependence. For value of r less than r_1, the axial pressure displays a strong interference effects, suggesting that the acoustic field close to the piston is complicated. The distance r_1 thus serves as a convenient demarcation between the complicated near field found close to the source and the simpler far field found at large distances from the source. The quantity r_1 has physical meaning only if the ratio a/λ is large enough so that r_1 is positive. In deed, if a = $\lambda/2$ then r_1 is zero and there is no near field.

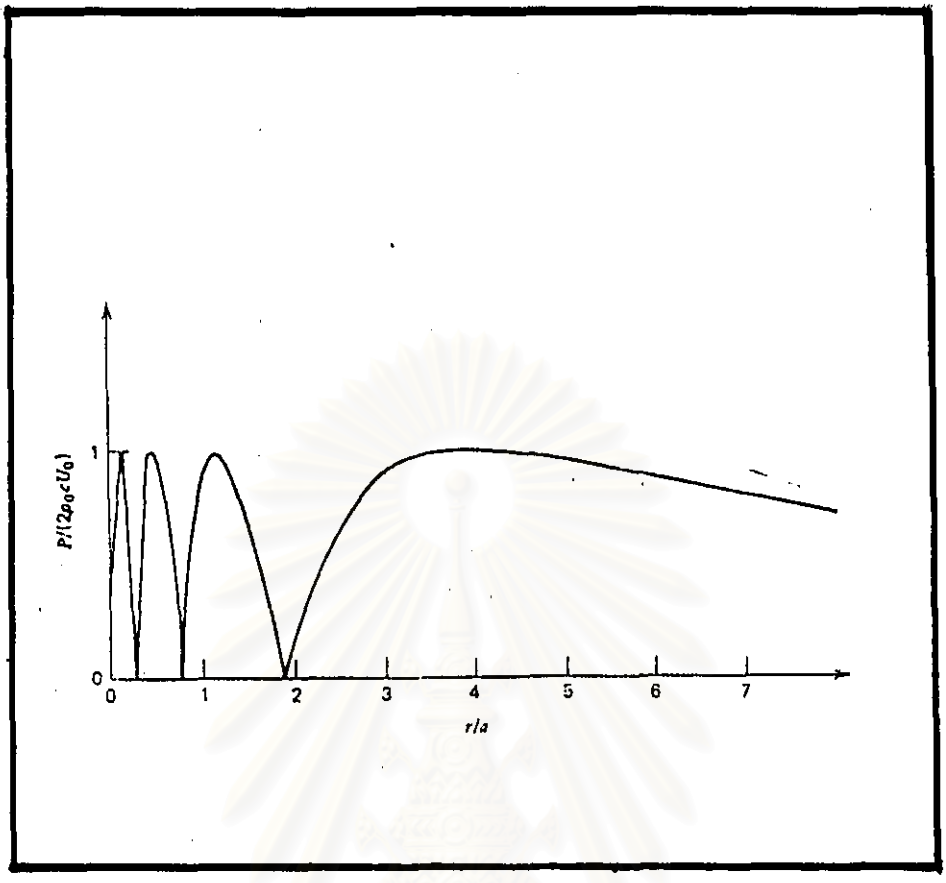

Figure 3-12: On-axis response of a circular plane piston with $a/\lambda = 4$